Applied Materials Today 9 (2017) 402–406

Contents lists available at ScienceDirect

Applied Materials Today

journal homepage: www.elsevier.com/locate/apmt

Polymer-assisted deposition of $SrTiO_3$ film as cathode buffer layer in inverted polymer solar cells

Haizhen Wang [a], Brian Patterson [a], Jianzhong Yang [b], Di Huang [a], Yang Qin [b], Hongmei Luo [a,*]

[a] Department of Chemical and Materials Engineering, New Mexico State University, Las Cruces, NM 88003, United States
[b] Department of Chemistry and Chemical Biology, University of New Mexico, Albuquerque, NM 87131, United States

ARTICLE INFO

Article history:
Received 8 June 2017
Received in revised form 22 August 2017
Accepted 8 September 2017

Keywords:
Polymer-assisted deposition
$SrTiO_3$ film
Buffer layer
Inverted polymer solar cells

ABSTRACT

Polymer-assisted deposition (PAD) method has been employed to prepare $SrTiO_3$(STO) films on ITO substrates, which have been applied as cathode buffer layer in inverted polymer solar cells. ZnO and TiO_2 films on ITO glass were also prepared via PAD and have been utilized as cathode buffer layers in the inverted polymer solar cells for comparison, which show better efficiency than those using ZnO and TiO_2 as interfacial layers prepared through other methods. The power conversion efficiency (PCE) of ~3.5% was achieved with STO as the cathode buffer layer as well as MoO_3 as the anode buffer layer, which is comparable to that with ZnO and TiO_2 prepared using the same method as cathode buffer layers. Our findings indicate that STO has the potential to be a candidate as interfacial layers in solar cell devices.

1. Introduction

Polymer solar cells (PSCs) have attracted great attention due to their potential applications as low-cost renewable energy sources [1–3]. Conventional PSCs usually consist of an active layer (including electron transport layer, absorber layer and hole transport layer such as poly(3,4-ethylenedioxythiophene) polystyrene sulfonate (PEDOT:PSS)) sandwiched by transparent indium tin oxide (ITO) on glass as the anode and a low-work-function metal (typically aluminum) as the cathode. Anode degradation caused by the PEDOT diffusion induced etching of ITO can occur in conventional PSCs, resulting in short lifetime of the devices [4–6]. In order to enhance the stability of PSCs, PSCs of inverted structures, where the nature of charge collection is reversed, have been employed as an alternative to improve the lifetime of solar cells [7–9]. To further enhance the device stability, inorganic semiconductor oxides inserted between ITO and the active layer has been implemented as a buffer layer in an inverted device structure to selectively collect electrons as well as avoid the contact of ITO film with PEDOT polymer [4,6,8–10]. The buffer layer works as an electron-collecting electrode and a hole-blocking layer, which is essential for achieving high efficiency PSCs [11]. Due to their matching band structures, excellent physical properties and high carrier mobility, several transitional metal oxides, such as zinc oxide (ZnO) [5,8,12,13], titanium oxide (TiO_2) [6,9,14], niobium oxide (Nb_2O_5) [9] have been utilized as the electron transport layer in contact with the conjugated polymers (commonly poly(3-hexylthiophene) (P3HT) with [6,6]-phenyl-C61-butyric acid methyl (PCBM)) in the inverted PSCs to replace PEDOT in order to achieve a higher stability.

In terms of the preparation of metal oxide films, a variety of approaches have been developed, including sol–gel [15], hydrothermal [14,16–19], chemical vapor deposition (CVD) [20], pulsed laser deposition (PLD) [21], etc. Polymer-assisted deposition (PAD), an aqueous chemical solution route, has paved a new path for film growth since it was first reported in 2004 [22]. In such growth method, polymers used as binding agent to metal ions play critical roles in growing high-quality thin films. Polymers could almost combine with any metal ions by electrostatic attraction, hydrogen bonding or covalent bonding to form metal–polymer complexes. This indicates that it is possible to prepare almost any kind of metal–polymer complex solutions which could not be realized through other chemical solution method. Besides, the viscosity of the metal–polymer complexes could also be adjusted through controlling the amount of polymer added, which would further affect the film thickness or even quality. Moreover, films prepared by PAD method are uniform and smooth with high quality since the material growth could be controlled on the molecular level by preventing the metal hydrolysis through forming stable and environmentally friendly metal–polymer precursors [22,23]. Films for different materials, such as metal oxides [24,25], metal-nitrides [26–28] and metal-carbides [29,30] have been successfully obtained by using this method.

* Corresponding author.
E-mail address: hluo@nmsu.edu (H. Luo).

http://dx.doi.org/10.1016/j.apmt.2017.09.004
2352-9407/

$SrTiO_3$ with the perovskite structure is a very attractive material for application in microelectronics because of its high-charge storage capacity, chemical stability, good insulating properties and excellent optical transparency in the visible region [31]. It has a similar band structure as ZnO but a higher dielectric constant ($\sim 10^4$) [10], which can favor charge transfer and thus be potentially used as electron transport layer in PSCs. $SrTiO_3$/ZnO composites with different mixing ratios used as cathode buffer layer have been demonstrated in inverted PSCs [10]. The power conversion efficiency of PSCs with STO:ZnO as electron transport layer varies significantly depending on the ratio of STO to ZnO. With the ratio of STO to ZnO increasing, the power conversion efficiency first increases and then decreases with a maximum efficiency of 4.1% when the ratio of STO to ZnO is 1:9. When the ratio increases to 1:3, the power conversion efficiency decreases to 2.38%. However, the mixing of those two composites increases the complexity of the material preparation and introduces extra grain boundaries, which is detrimental to the electron transport and thus the power conversion efficiency of the PSCs.

Here, we report on the inverted PSCs with pure $SrTiO_3$films as cathode buffer layer for the first time. Uniform $SrTiO_3$ films were fabricated on ITO substrate via the PAD method to work as cathode buffer layer in the inverted PSCs. The results indicate that the power conversion efficiency of the solar cells based on P3HT and PCBM with $SrTiO_3$ film as cathode buffer layer and MoO_3 as anode interfacial layer is up to 3.5%, comparable to that of PSCs with ZnO as buffer layer reported previously [5,8,12,13].

2. Experimental

2.1. Preparation of strontium titanium oxide (STO) film and powder by PAD

A stable strontium–polymer solution was prepared by dissolving strontium nitrate (2 g), polyethyleneimine (PEI 4 g, 50 wt% PEI in water), and ethylenediaminetetraacetic acid (EDTA, 2 g) in 30 ml deionized (DI) water. Titanium–polymer solution was prepared by mixing 3 ml titanium chloride solution (1 M in toluene) with 15 ml hydrogen peroxide (H_2O_2) with addition of PEI (10 g, 50 wt% PEI in water), EDTA (5 g) and extra deionized water. Then two metal–polymer solutions were mixed to get equal molar amount of strontium and titanium in the resultant mixture, which was further stirred for 4 h. Then the solution was spin-coated on the ITO-coated glass or fluorine tin oxide (FTO)-coated glass at a speed of 2500 rpm for 30 s. Finally, the films were annealed at 550 °C for 30 min in air with a ramp rate of 1 °C/min. STO powder was also prepared using exactly the same procedure without spin-coating step. For comparison, ZnO and TiO_2films were prepared using PAD method according to previous reports on the metal–polymer precursors [32,33], and spin-coating and annealing were same as STO films.

2.2. Device fabrication

To fabricate ITO/STO/P3HT:PCBM/Al structures, the ITO substrates were first cleaned in an ultrasonic bath with acetone, isopropanol, and DI-water each for 15 min sequentially followed by oxygen plasma treatment for 1 min. The metal–polymer precursor solution was spin-coated on cleaned ITO substrates at 2500 rpm for 30 s followed by heating at 550 °C for 30 min in air to form the STO layer. Second, the active layer of P3HT:PCBM was spin-coated on the STO layer at a speed of 700 rpm for 60 s in the glove box and then the devices were thermally annealed at 150 °C for 10 min. Finally, the Al (100 nm) layer was evaporated onto the resultant structures of the devices. For comparison, PSCs with ZnO and TiO_2 films prepared via PAD replacing the STO layer as the charge transport layer were also fabricated using the same procedure mentioned above.

To further investigate the performance of STO as cathode buffer layer, another device structure (ITO/STO/P3HT:PCBM/MoO_3/Al) was also fabricated. All the fabrication procedure was exactly the same as the previous structure except that 6 nm MoO_3 was thermally evaporated with a base pressure of about 1×10^{-6} Torr before Al was deposited.

2.3. Characterization

The structure, composition and morphology of the samples were characterized by X-ray diffraction (XRD) and atomic force microscopy (AFM). XRD was carried out in Rigaku Miniflex-II with Cu Ka (λ = 1.5406 Å) radiation, 30 kV/15 mA current and kβ-filter. AFM was performed in a Dimension Fast Scan Atomic Force Microscopy by Bruker Corporation with tapping mode. The current density (J)–voltage (V) characteristics of the solar cells were measured in the glove box using a Keithley 2400 source measurement unit, and an Oriel Xenon lamp (450 W) coupled with an AM1.5 filter. A calibrated silicon reference solar cell certified by the National Renewable Energy Laboratory (NREL) was used to verify the measurement conditions. A light intensity of 100 mW/cm^2 was used in all the measurements in this study.

3. Results and discussion

The structure of the as-synthesized STO powder was characterized by XRD, as shown in Fig. 1a. All the diffraction peaks of the sample could be assigned to cubic-phase with calculated lattice parameter of a = 3.9027 Å, which are well in agreement with the reported values (PDF card #35-0734). No other peaks were observed, which indicates that the phase of the as-synthesized material is very pure. All the peaks are identifiable with high intensities, indicating the excellent crystalline quality of the material.

AFM images show that the as-synthesized STO film surface is uniform and flat (Fig. 1b and c). The relatively uniform surface could be further confirmed by the three-dimensional graph. The root

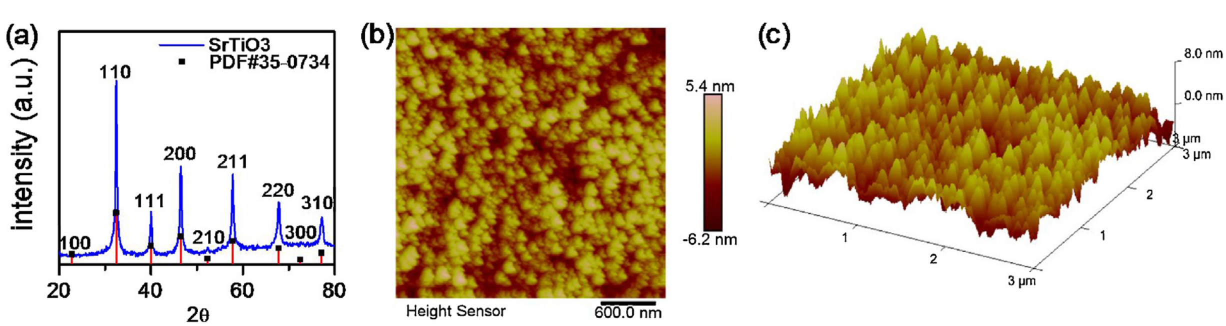

Fig. 1. XRD pattern of the as-synthesized STO powder (a) and AFM surface morphology (b, c) of STO film.

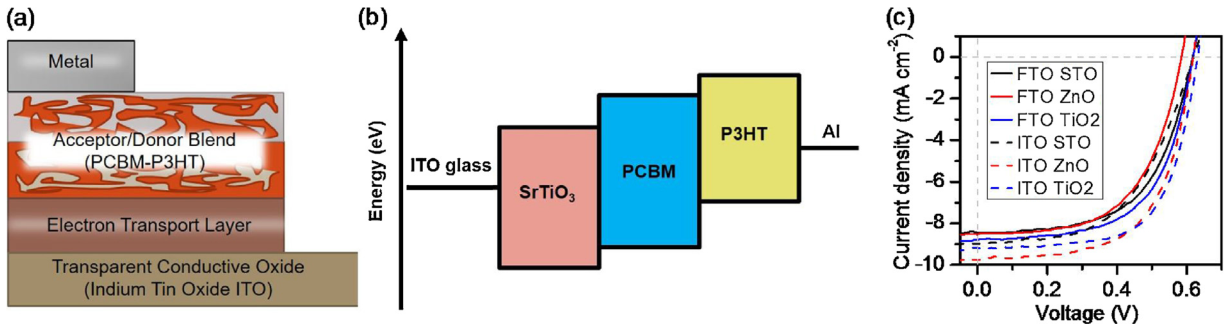

Fig. 2. (a) Schematic of inverted structure of PSCs we adopted; (b) energy band alignment diagram for the inverted structure; and (c) the *J–V* curves of the inverted PSCs with STO, TiO_2, ZnO on ITO and FTO glass as cathode buffer layers.

Table 1
J–V characteristics of STO, TiO_2, ZnO on ITO and FTO-glass as cathodic buffer layers for the inverted polymer solar cells.

	V_{oc} (V)	J_{sc} (mA/cm^2)	FF	PCE (%)
ITO/STO	0.619465	8.990258	0.531512	**2.960068**
ITO/ZnO	0.618167	9.744184	0.614077	3.698911
ITO/TiO_2	0.630859	9.186875	0.651412	3.775338
FTO/STO	0.616843	8.436181	0.589181	**3.065977**
FTO/ZnO	0.584837	8.523768	0.577973	2.881207
FTO/TiO_2	0.617673	8.800226	0.600575	3.234525

mean square (RMS) surface roughness is around 1.76 nm, which is much smaller than that of cathode buffer layers reported previously [10]. It is anticipated that the buffer layer with small roughness could lead to a good contact with the polymer, which could benefit the electron transport at the interface between the buffer layer and polymer, thus resulting in solar cell with a low series resistance and higher short-circuit current [4].

The as-prepared STO film on ITO substrate has been applied as electron transport layer in the inverted PSCs constructed with a blend of P3HT and PCBM (Fig. 2a). The corresponding energy band diagram is displayed in Fig. 2b, which indicates that the STO layer would allow electrons to be efficiently collected by the cathode. Fig. 2c represents the characteristic *J–V* plot. The short-circuit current density (J_{sc}), open-circuit voltage (V_{oc}), fill factor (FF), and power conversion efficiency (PCE) values are summarized in Table 1. It was observed that PSCs with STO as cathode buffer layer has a PCE of 2.96%.

ZnO and TiO_2 have drawn much attention in serving as the buffer layers because they have good transparency across the whole visible spectral range, relatively high-electron mobility and environmental stability [5,34]. Since this is the first time for pure STO to be used as electron transport layer in PSCs, we also included the data that ZnO and TiO_2 thin films prepared by the same method used as electron transport layer in PSCs for comparison. Therefore, ZnO and TiO_2 films were also fabricated using PAD method and have been utilized as the cathode buffer layer in the inverted PSCs with the same structure. To compare with the PSCs with STO as cathodic buffer layer, while keeping all the other components measurement parameters the same (such as thickness of P3HT/PCBM, annealing process), we just changed the cathode buffer layer to ZnO and TiO_2 which have similar electron affinity and band gap with STO. From the results in Fig. 2c and Table 1, we can see that PSCs with STO as cathode buffer layer give the comparable PCE compared with those using well-developed ZnO and TiO_2 as cathode buffer layers. In addition, PSCs with PAD prepared TiO_2 and ZnO as electron transport layers exhibit relatively higher efficiencies than those synthesized via other methods, which is shown in Table 2. This indicates that PAD method has the potential to be a versatile method for preparation of metal oxide films as cathode buffer layers in polymer solar cells. Furthermore, we also investigated how the substrates influence the performance of the PSCs by replacing the ITO substrate with FTO glass while keeping all other parameters the same. Overall, the PSCs performances are comparatively better with ITO as substrate than those with FTO as substrate, except for STO films whose performances are similar by using these two different substrates, indicating that STO can be used as cathode buffer layer with less requirement for the substrate selection.

Molybdenum oxide (MoO_3) film prepared using PAD method has been reported as anode buffer layer in inverted PSCs which would benefit the hole extraction and thus exhibits great performance with PCE of 2.94% [22]. Considering that with STO as cathode buffer layer, the performance of PSCs has been improved and the structure could also be stabilized. Therefore, it is anticipated when we applied both MoO_3 as anode and STO as cathode interfacial layers in the inverted PSCs, the performance could be further enhanced. We have designed another inverted PSC structure with both anode and cathode buffer layers as shown in Fig. 3a and the corresponding energy level diagram in this structure is also illustrated in Fig. 3b. Fig. 3c indicates the characteristic *J–V* plot, from which it is shown that the inverted polymer solar cell performance could be refined with values of V_{oc} = 0.49 V, J_{sc} = 15.1 mA/cm^2, and

Table 2
Comparison of the inverted PSC performances using ZnO and TiO_2 as cathode buffer layers prepared by PAD and other methods.

Material	Methods	V_{oc} (V)	J_{sc} mA/cm^2)	FF	PCE (%)	Ref
ITO/TiO_2/P3HT/PEDOT:PSS/Au	Hydrothermal	0.63	8.12	0.61	3.12	[16]
ITO/ZnO-TiO_2/P3HT:PCBM/Ag	ZnO template	0.646	9.95	0.516	3.32	[35]
ITO/ZnOTiO_2/P3HT/Au	Sol–gel	0.46	3.48	0.47	0.76	[15]
ITO/TiO_2/P3HT:PCBM/LiF/Al	Hydrothermal	0.68	8.0	0.6	3.2	[19]
ITO/TiO_2/P3HT:PCBM/Al	PAD	0.631	9.19	0.65	3.775	Our
ITO/ZnO/PCBM:P3HT/Ag	Sol–gel	0.556	11.22	0.475	2.58	[36]
ITO/ZnO/PCBM:P3HT/Ag	Sol–gel	0.475	10.00	0.475	2.0	[13]
ITO/ZnO/PCBM:P3HT/Ag	Sol–gel	0.57	9.60	0.50	2.7	[12]
ITO/ZnO/PCBM: P3HT/Al	PAD	0.618	9.744	0.61	3.699	Our

The power conversion efficiency of solar cells with STO on ITO/FTO two different substrates as cathode buffer layers has been highlighted to compare with that with different buffer layers.

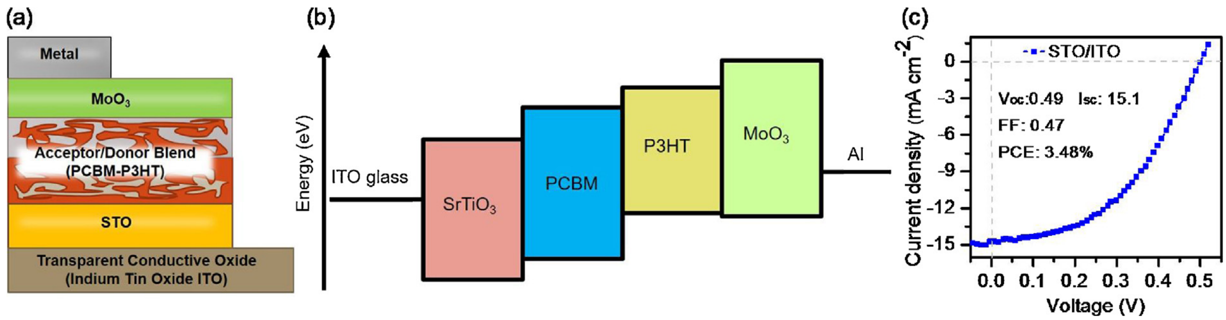

Fig. 3. (a) Inverted structure of PSCs with both cathode and anode buffer layers; (b) schematic energy band diagram of the devices; and (c) *J*–*V* characteristics of the inverted PSC with STO film as the cathodic buffer layer and MoO_3 as anode buffer layer.

FF = 47%. The relatively low fill factor may be due to the series resistance in the solar cell [4], which is believed to be the dominant factor limiting the PCE here. The power conversion efficiency with STO and MoO_3 as cathode and anode buffer layers could achieve ~3.5%, which is comparatively high in the inverted polymer solar cell structures [6,13,15,16,36]. The high conversion efficiency might be attributed to the efficient electron transport in STO film, which could stretch into P3HT–PCBM polymers to extract electrons. We expect that with further optimizing the device structures, the PCE of this PSC could be further advanced.

4. Conclusion

STO films have been prepared using PAD method and exhibit good quality with low roughness. When STO was applied as cathode buffer layer in the inverted polymer solar cell, the power conversion efficiency was 2.96%. Further incorporation MoO_3 as anode buffer layer in inverted PSC, the efficiency could be improved to 3.48%. Our findings provide a low-cost solution-processable method to synthesize new cathode buffer layer material STO with fairly good performance. In view of the long stability and high dielectric constant, the PCE of PSCs with STO as cathode buffer layer would be expected to be further improved with the optimized device structures.

Acknowledgements

We thank the support from New Mexico EPSCoR with NSF-1301346. We also thank Dr. Gen Chen and Prof. Guozhong Cao for their support and valuable suggestions.

References

[1] J.-L. Lan, S.-J. Cherng, Y.-H. Yang, Q. Zhang, S. Subramaniyan, F.S. Ohuchi, S.A. Jenekhe, G. Cao, The effects of Ta_2O_5–ZnO films as cathodic buffer layers in inverted polymer solar cells, J. Mater. Chem. A2 (2014) 9361–9370.
[2] Y.-H. Chang, S.-R. Tseng, C.-Y. Chen, H.-F. Meng, E.-C. Chen, S.-F. Horng, C.-S. Hsu, Polymer solar cell by blade coating, Org. Electron. 10 (2009) 741–746.
[3] W.-H. Baek, H. Yang, T.-S. Yoon, C.J. Kang, H.H. Lee, Y.-S. Kim, Effect of P3HT:PCBM concentration in solvent on performances of organic solar cells, Sol. Energy Mater. Sol. C 93 (2009) 1263–1267.
[4] J.J. Tian, G.Z. Cao, Design, fabrication and modification of metal oxide semiconductor for improving conversion efficiency of excitonic solar cells, Coord. Chem. Rev. (2016) 193–215.
[5] Z.Q. Liang, Q.F. Zhang, O. Wiranwetchayan, J.T. Xi, Z. Yang, K. Park, C.D. Li, G.Z. Cao, Effects of the morphology of a ZnO buffer layer on the photovoltaic performance of inverted polymer solar cells, Adv. Funct. Mater. 22 (2012) 2194–2201.
[6] O. Wiranwetchayan, Q.F. Zhang, X.Y. Zhou, Z.Q. Liang, P. Singjai, G.Z. Cao, Impact of the morphology of TiO_2 films as cathode buffer layer of the efficiency of inverted-structure polymer solar cells, Chalcogenide Lett. 9 (2012) 157–163.
[7] M. Shan, S. Wang, Z. Bian, J. Liu, Y. Zhao, Hybrid inverted organic photovoltaic cells based on nanoporous TiO_2 films and organic small molecules, Sol. Energy Mater. Sol. C 93 (2009) 1613–1617.
[8] Z.Q. Liang, Q.F. Zhang, L. Jiang, G.Z. Cao, ZnO cathode buffer layers for inverted polymer solar cells, Energy Environ. Sci. (2015) 3442–3476.
[9] O. Wiranwetchayan, Z. Liang, Q. Zhang, G. Cao, P. Singjai, The role of oxide thin layer in inverted structure polymer solar cells, Mater. Sci. Appl. 2 (2011) 1697.
[10] J.-L. Lan, Z.Q. Liang, Y.-H. Yang, F.S. Ohuchi, S.A. Jenekhe, G.Z. Cao, The effect of $SrTiO_3$:ZnO as cathodic buffer layer for inverted polymer solar cells, Nano Energy 4 (2014) 140–149.
[11] J.-P. Liu, K.-L. Choy, X.-H. Hou, Charge transport in flexible solar cells based on conjugated polymer and ZnO nanoparticulate thin films, J. Mater. Chem. 21 (2011) 1966–1969.
[12] K. Takanezawa, K. Hirota, Q.-S. Wei, K. Tajima, K. Hashimoto, Efficient charge collection with ZnO nanorod array in hybrid photovoltaic devices, J. Chem. Phys. C111 (2007) 7218–7223.
[13] D.C. Olson, J. Piris, R.T. Collins, S.E. Shaheen, D.S. Ginley, Hybrid photovoltaic devices of polymer and ZnO nanofiber composites, Thin Solid Films 496 (2006) 26–29.
[14] J.T. Xi, O. Wiranwetchayan, Q.F. Zhang, Z.Q. Liang, Y.M. Sun, G.Z. Cao, Growth of single-crystalline rutile TiO_2 nanorods on fluorine-doped tin oxide glass for organic–inorganic hybrid solar cell, J. Mater. Sci: Mater. Electron. 23 (2012) 1657–1663.
[15] Y. Li, P. Lu, M. Jiang, R. Dhakal, P. Thapaliya, Z. Peng, B. Jha, X. Yan, Femtosecond time-resolved fluorescence study of TiO_2-coated ZnO nanorods/P3HT photovoltaic films, J. Chem. Phys. C116 (2012) 25248–25256.
[16] W.-P. Liao, S.-C. Hsu, W.-H. Lin, J.-J. Wu, Hierarchical TiO_2 nanostructured array/P3HT hybrid solar cells with interfacial modification, J. Chem. Phys. C116 (2012) 15938–15945.
[17] S.-C. Hsu, W.-P. Liao, W.-H. Lin, J.-J. Wu, Modulation of photocarrier dynamics in indoline dye-modified TiO_2 nanorod array/P3HT hybrid solar cell with 4-tert-butylpridine, J. Chem. Phys. C116 (2012) 25721–25726.
[18] W.-P. Liao, J.-J. Wu, Efficient electron collection in hybrid polymer solar cells: in-situ-generated ZnO/poly(3-hexylthiophene) scaffolded by a TiO_2 nanorod array, J. Chem. Phys. Lett. 4 (2013) 1983–1988.
[19] P. Yang, X. Zhou, G. Cao, C.K. Luscombe, P3HT:PCBM polymer solar cells with TiO_2 nanotube aggregates in the active layer, J. Mater. Chem. 20 (2010) 2612–2616.
[20] T.F. Chen, A.J. Wang, L.Y. Kong, Y.L. Li, Y.S. Wang, Growth and properties of Cl^- incorporated ZnO nanofilms grown by ultrasonic spray-assisted chemical vapor deposition, J. Nanosci. Nanotechnol. 16 (2016) 3669–3673.
[21] Y. Xu, Q. Zhou, H.M. Luo, Effect of crystallinity on lithium ion storage behavior of TiO_2 thin films prepared by pulsed laser deposition, Chem. Eng. (2016) 11–18.
[22] Q.H. Yi, P.F. Zhai, Y.H. Sun, Y.H. Lou, J. Zhao, B.Q. Sun, B. Patterson, H.M. Luo, W.R. Zhang, L. Jiao, H.Y. Wang, G.F. Zou, Aqueous solution-deposited molybdenum oxide films as an anode interfacial layer for organic solar cells, ACS Appl. Mater. Int. 7 (2015) 18218–18224.
[23] G.F. Zou, J. Zhao, H.M. Luo, T.M. McCleskey, A.K. Burrell, Q.X. Jia, Polymer-assisted-deposition: a chemical solution route for a wide range of materials, Chem. Soc. Rev. 42 (2013) 439–449.
[24] L. Fei, L.Y. Zhu, X.M. Cheng, H.Y. Wang, S.M. Baber, J. Hill, Q.L. Lin, Y. Xu, S.G. Deng, H.M. Luo, Structure and magnetotransport properties of epitaxial nanocomposite $La_{0.67}Ca_{0.33}MnO_3$:$SrTiO_3$ thin films grown by a chemical solution approach, Appl. Phys. Lett. 100 (2012) 082403.
[25] H. Luo, H. Yang, S.A. Baily, O. Ugurlu, M. Jain, M.E. Hawley, T.M. McCleskey, A.K. Burrell, E. Bauer, L. Civale, Self-assembled epitaxial nanocomposite $BaTiO_3$–$NiFe_2O_4$ films prepared by polymer-assisted deposition, J. Am. Chem. Soc. 129 (2007) 14132–14133.
[26] Z. Hui, X. Tang, D. Shao, H. Lei, J. Yang, W. Song, H. Luo, X. Zhu, Y. Sun, Epitaxial antiperovskite superconducting $CuNNi_3$ thin films synthesized by chemical solution deposition, Chem. Commun. 50 (2014) 12734–12737.
[27] H. Luo, H. Wang, Z. Bi, D.M. Feldmann, Y. Wang, A.K. Burrell, T.M. McCleskey, E. Bauer, M.E. Hawley, Q. Jia, Epitaxial ternary nitride thin films prepared by a chemical solution method, J. Am. Chem. Soc. 130 (2008) 15224–15225.
[28] H. Luo, H. Wang, Z. Bi, G. Zou, T.M. McCleskey, A.K. Burrell, E. Bauer, M.E. Hawley, Y. Wang, Q. Jia, Highly conductive films of layered ternary transition-metal nitrides, Angew. Chem. Int. Ed. 48 (2009) 1490–1493.

[29] G.F. Zou, H. Wang, N. Mara, H.M. Luo, N. Li, Z. Di, E. Bauer, Y. Wang, T. McCleskey, A. Burrell, Chemical solution deposition of epitaxial carbide films, J. Am. Chem. Soc. 132 (2010) 2516–2517.
[30] G.F. Zou, H.M. Luo, Y. Zhang, J. Xiong, Q. Wei, M. Zhuo, J. Zhai, H. Wang, D. Williams, N. Li, A chemical solution approach for superconducting and hard epitaxial NbC film, Chem. Commun. 46 (2010) 7837–7839.
[31] A.C.L.S. Marques, Advanced Si pad detector development and $SrTio_3$ studies by emission channeling and hyperfine interaction experiments, PhD thesis, Universidade de Lisboa. Faculdade de Ciências, 2009.
[32] Q.X. Jia, T.M. McCleskey, A.K. Burrell, Y. Lin, G.E. Collis, H. Wang, A.D. Li, S.R. Foltyn, Polymer-assisted deposition of metal-oxide films, Nature Mater. 3 (2004) 529–532.
[33] Y. Lin, J. Xie, H. Wang, Y. Li, C. Chavez, S. Lee, S. Foltyn, S. Crooker, A. Burrell, T. McCleskey, Green luminescent zinc oxide films prepared by polymer-assisted deposition with rapid thermal process, Thin Solid Films 492 (2005) 101–104.
[34] Y.W. Heo, D. Norton, L. Tien, Y. Kwon, B. Kang, F. Ren, S. Pearton, J. LaRoche, ZnO nanowire growth and devices, Mater. Sci. Eng. R: Rep. 47 (2004) 1–47.
[35] S. Yodyingyong, X. Zhou, Q. Zhang, D. Triampo, J. Xi, K. Park, B. Limketkai, G. Cao, Enhanced photovoltaic performance of nanostructured hybrid solar cell using highly oriented TiO_2 nanotubes, J. Chem. Phys. C114 (2010) 21851–21855.
[36] M.-S. White, D. Olson, S. Shaheen, N. Kopidakis, D.S. Ginley, Inverted bulk-heterojunction organic photovoltaic device using a solution-derived ZnO under layer, Appl. Phys. Lett. 89 (2006) 143517.